Z. Phys. C – Particles and Fields 38, 51–57 (1988)

Zeitschrift für Physik C Particles and Fields

Charged particle spectra in ^{16}O induced nuclear collisions at the CERN SPS*

I. Lund
GSI, Darmstadt, Federal Republic of Germany

WA 80 Collaboration

R. Albrecht[1], T.C. Awes[2], C. Baktash[2], P. Beckmann[3], F. Berger[3], R. Bock[1], G. Claesson[1], L. Dragon[3], R.L. Ferguson[2], A. Franz[4], S.I.A. Garpman[5], R. Glasow[3], H.Å. Gustafsson[5,c], H.H. Gutbrod[1], J.W. Johnson[2], K.–H. Kampert[3], B.W. Kolb[1], P. Kristiansson[4], I.Y. Lee[2], H. Löhner[3], I. Lund[1,a], F.E. Obenshain[2], A. Oskarsson[5], I. Otterlund[5], T. Peitzmann[3], S. Persson[5], F. Plasil[2], A.M. Poskanzer[4], M. Purschke[3], H.G. Ritter[4], R. Santo[3], H.R. Schmidt[1], T. Siemiarczuk[1,b], S.P. Sorensen[2,d], E. Stenlund[5], G.R. Young[2]

[1] Gesellschaft für Schwerionenforschung (GSI), D-6100 Darmstadt, Federal Republic of Germany
[2] Oak Ridge National Laboratory, Oak Ridge, TN 37831, USA
[3] University of Münster, D-4400 Münster, Federal Republic of Germany
[4] Lawrence Berkeley Laboratory, Berkeley, CA 94720, USA
[5] Division of Cosmic and Subatomic Physics, University of Lund, S-22362 Lund, Sweden

Abstract. Charged particle multiplicity distributions and pseudo-rapidity density distributions from ^{16}O induced nuclear collisions at 200 and 60 A GeV are presented. The data were taken, using a minimum-bias trigger, with the WA 80 set-up at the CERN SPS. In this presentation we focus on how the yield of charged particles depends on the projectile energy, the mass number of the target nucleus and the energy measured in a uranium-plastic sampling calorimeter covering angles close to zero degrees. The data are compared to simulations from the event generator FRITIOF.

Introduction

The CERN SPS programme of fixed-target nucleus-nucleus collisions at ultrarelativistic energies started in 1986 with successful runs that used beams of ^{16}O nuclei at 60 A GeV and 200 A GeV. The goals of this programme are manifold. We hope to study nuclear matter under the conditions of high compression and temperature that might be obtained in these collisions and to extract information about the equation of state for the nuclear medium. In the case of high 4-momentum transfer, the relevant constituents of the nucleus are the coloured quarks. This fact implies that, nuclear physics at these energies cannot be fully understood without accounting for the basic reaction mechanisms of quarks and gluons [1]. The ultimate goal of the programme is to search for the predicted deconfinement phase-transition from excited nuclear matter to quark-gluon plasma. Here we present first results regarding charged particle production in oxygen-nucleus collisions as measured by the WA 80 experiment [2].

Experimental set-up

The data were taken with the WA 80 experimental set-up [3] (See Fig. 1) using the ^{16}O beams at 200 and 60 A GeV delivered from the CERN SPS in November 1986. A typical beam level was 2×10^6 ions per beam spill, where the effective spill length was about 3.8 s per machine cycle of 14.4 s. The ^{16}O ions were identified with quartz Cherenkov beam counters before they impinged on targets of C, Cu, Ag and

* Presented at the 6th International Conference on Ultra-Relativistic Nucleus-Nucleus Collisions – Quark Matter 1987, 24–28 August 1987, Nordkirchen, Federal Republic of Germany

[a] Post Doctoral Fellowship from Swedish Natural Science Research Council
[b] On leave of absence from the Institute for Nuclear Studies, PL-00681 Warsaw, Poland
[c] EP-Division, CERN, CH-1211 Geneva, Switzerland
[d] University of Tennessee, Knoxville, TN 37996, USA

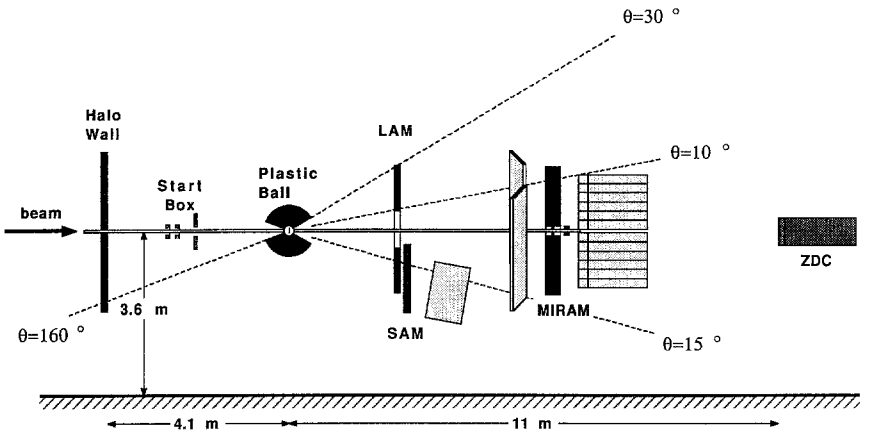

Fig. 1. A schematic view of the WA80 set-up. The detectors used in this analysis are marked in a darker grey colour. The different abbreviations are explained in the text

Au which were about 200 mg cm^{-2} thick. The vacuum system was extended 6 m downstream from the 600 μm thick aluminium target-chamber by a 5-cm-diameter carbon-fibre/epoxy beam pipe of 500-μm nominal thickness. A uranium-plastic sampling calorimeter, the Zero-Degree Calorimeter (ZDC) [4], measured the energy of beam particles and reaction products within $\theta < 0.3°$ at a distance of 11 m from the target. Since it is believed that the major part of the energy flux within this polar angle is due to spectator fragments and nucleons not participating in the reaction, this allowed us to measure the degree of "centrality" of the reaction. The data were taken with a minimum-bias trigger which required:

1) the measured energy in ZDC to be less than 88% of the total projectile energy;

2) at least one charged particle to be recorded within a polar angle of $1° < \theta < 30°$.

In the angular range $30° < \theta < 160°$ the charged particles were measured by 655 $\Delta E/E$ (CaF_2/plastic) scintillator telescopes. This detector, the Plastic Ball [5], was in operation for five years at the LBL Bevalac before it was moved to CERN early in 1986.

A unique feature of the WA80 set-up is the nearly 4π sr (97%) coverage for measurements of charged particles. Beyond the range of Plastic Ball, this coverage is provided by a set of Iarrocci streamer-tube arrays using pad read-out [6]. At a distance of about 2.4 m from the target the Large-Angle Multiplicity Detector (LAM) covers the polar angles between 10 and 30 degrees. The Saphir Multiplicity Detector (SAM), located at 2.6 m from the target, covers the angles $\theta = 20° \pm 10°$ and $\Delta\phi = 80°$ below the beam line. The Mid-Rapidity Multiplicity Detector (MIRAM) is situated at a distance of about 6.0 m from the target. It consists of two identical streamer-tube detector planes which cover the polar angles between 1° and 13°. The pad sizes vary from 1.0×2.6 to 3.5×5.2 cm^2 depending on their distance to the beam line and the detector plane in question. The total number of pads used in the read-out system for the streamer-tube detectors amounts to more than 29,000.

Analysis and corrections to the data

In this analysis we have used from the Plastic Ball detector, only the information whether or not a module was hit by a charged particle. The contribution to the charged particle yield, in the angular region covered by the Plastic Ball detector, from γ conversion and secondary hadronic interactions is estimated to be less than 1.5% and this has not been corrected for. The only applied correction to the data taken by the Plastic Ball is that for multiple hits of charged particles. The charged particle multiplicity and angular distributions were first recorded from raw data. The multiplicity distribution was then corrected in an approximate way in order to compensate for the loss due to the effect of multiple hits. With this information as input, and assuming azimuthal symmetry and no correlations among the particles in an event, we constructed Monte Carlo events which were subsequently run through a simulation using the geometrical layout of the Plastic Ball detector. From this simulation the "true" multi-hit probability was determined. The applied correction is typically of the order of 5 to 30% in the polar angular region $30° < \theta < 60°$ and is less than 5% for $\theta > 60°$. In the angular region $30° < \theta < 35°$, for the very highest multiplicities (more than 140 modules firing in the Plastic Ball), the correction reaches values of 40 to 50%.

A charged particle traversing a streamer-tube detector can start a streamer which is sensed by more than one pad. The "fired" pads in one detector plane therefore have to be examined using a cluster routine

in order to decide how many of them should be assigned to one "hit". As a first step we assigned all nearby fired pads to one hit. Using the data for $^{16}O + ^{197}Au$ interactions at 200 A GeV we obtained (after averaging over the different pad sizes) 60% of the hits with only one fired pad, 22% with two fired pads, 8% with three "fired" pads and so on with decreasing probabilities. We have assumed that pad-configurations with more than four connected pads are produced by at least two charged particles and have split up these into more probable geometrical configurations.

In order to reduce the background of particles from secondary interactions we have correlated the hits in the two MIRAM detector planes before we counted the charged particles. This has also been done in the angular region where LAM and SAM have an overlap. In the part of LAM where it is not possible to correlate the recorded hits with the hits from the other detector planes, we have reduced the yield by a polar-angle dependent factor which was determined from the correlations between LAM and SAM. This factor is typically of the order of 10–15%.

The "efficiency" of the multiplicity detectors in detecting charged particles was determined by correlating the hits in the angular regions which are covered by three or more detector planes. The probability to detect a charged particle, averaged over the energy distribution of the particles, was estimated to be about 85% in each single plane. A second method of estimating the detection probability for charged particles, using plastic scintillator detectors positioned on both sides of a detector plane and averaging over different pad sizes and positions, also gave a value of around 85%. This figure includes the acceptance losses due to the lack of coverage of the detectors in between the streamer-tube channels and the less sensitive regions in between the read-out pads on the circuit boards. The efficiency corrections were made on a track-by-track basis. Each counted charged particle was assigned a weight of $(0.85)^{-2}$ or $(0.85)^{-1}$ depending on whether it was determined by correlating hits from two planes or not. The method employed for correcting the data for the inefficiency of the streamer-tube detectors was tested by applying it to different simulated distributions. For the lowest multiplicity values (say below multiplicity 8) it is found to create a bias which adds to the trigger bias in this region.

The multi-hit correction to the data taken with the streamer-tube detectors was determined in a manner similar to that used for the Plastic Ball detector. In the simulation, the inefficiency of the detector planes was taken into account and we also used the above-mentioned cluster routine. Usually, the correction due to the multi-hit probability is lower than 5%. However, for η values larger than 4.0 it reaches values up to 20%. One effect which this simulation also takes care of is the possibility of false correlations between hits from different detector planes in those angular regions where the particle density is high. If the incoming charged particle is seen in one plane but is missed in the other, a correlation could still be made with a nearby hit in the other plane. These "false" correlations can contribute as much as 10% to the yield of charged particles but usually contribute only a few percent. This effect has been corrected for.

When correcting for γ conversions in the aluminium target-chamber, the carbon/epoxy beam pipe, the air traversed and the streamer-tube detectors we have assumed that the π^0:s constitute one third of the total pion yield and that the relative numbers of produced pions, kaons and protons are given by [7]:

$$N_\pi : N_K : N_p = 15:2:1.$$

Due to the small average emission angle between the leptons created, the pair will, with very high probability, go through the same pad or two nearby pads (merged to one hit by the cluster routine) in the streamer-tube detectors and will therefore be counted as only one hit. The final correction for this effect falls from 4.4% at $\theta = 1.7°$ to 2.4% at $\theta = 8°$. It then stays small apart for the region where the MIRAM detector is shadowed by the LAM detector. In this region the correction is about 6%.

The last correction applied is for the increase in the yield of charged particles due to hadronic secondary interactions in the same materials as mentioned above. To calculate the number of particles emitted in the forward region we used a phenomenological model [8] and calculated the charged particle yield from pion-nucleus interactions at energies above 1 GeV. The slow, target-related fragments and hadrons that are produced in these collisions have been assumed to be rejected by the above-mentioned correlation criteria. We have also subtracted one leading hadron from the charged particles produced in each secondary interaction. The correction is about 7% at $\theta = 1.7°$ and then falls to below 1% at mid-rapidity values. Mainly this reflects, as is the case with the correction for γ conversion, the amount of material in the beam pipe traversed by the hadrons.

The charged particle contribution from decaying K^0_s:s and Λ:s is included in the data. In the FRITIOF event generator [9], used for the model calculations we will present, these decays were assumed to take place at the primary vertex. This contribution to the total yield of charged particles is estimated, with the help of the model events, to be 7%.

In this analysis we have used predictions from the event generator FRITIOF for comparisons with data. This model for nucleus-nucleus interactions is an extension of the Lund low-p_t hadron scattering model [10]. The WA80 minimum-bias trigger was simulated in the calculations when producing the distributions from the model events.

Experimental results

This analysis is based on 5000 events for each target and energy configuration. The data were taken with the trigger described above. The measured cross sections for the 200 A GeV minimum-bias data are 450, 1350, 1825 and 2475 mb for the targets C, Cu, Ag and Au, respectively. The corresponding values for the energy 60 A GeV are 650, 1675, 2250 and 2900 mb. The larger cross sections observed for the lower energy are mainly due to the fact that the nucleon-nucleon centre-of-mass system in this case is situated at a lower rapidity value in the laboratory system and consequently our minimum-bias trigger accepts a larger part of the total cross section.

In Fig. 2 we present the charged particle multiplicity distributions in the pseudo-rapidity ($\eta = -\ln tg(\theta/2)$) interval $-1.7 < \eta < 4.2$ for 200 A GeV ^{16}O interactions and different targets. For the lowest multiplicity values one clearly sees the onset of our trigger bias. Instead of rising, the cross sections reach a maximal value and then decrease. Since the carbon nucleus is smaller than the oxygen nucleus the bias is larger in the case of ^{16}O+C collisions. For the gold target we find a finite cross section for events with more than 450 charged particles. This value corresponds to more than 350 produced charged particles. For the heaviest targets we clearly see a slight rise in the charged particle yield before the sharp fall-off at higher multiplicities sets in. This feature is intuitively expected from a purely geometrical picture if one assumes that the average number of produced particles per participating nucleon is constant. Since the oxygen nucleus is smaller than the target nucleus all projectile nucleons can be assumed to be participants for the more "central" events. The cylindrical volume of the target nuclei which is passed by the projectile nucleons will then, apart from fluctuations, contain roughly the same number of nucleons when integrating over the different impact parameters. This feature will create a "bump" in the distribution before one reaches the region where, due to the fluctuations around the average events, the sharp fall-off of the cross section sets in. If you read off the multiplicities in Fig. 2 for which the cross sections have decreased to half the plateau values (this is indeed hazardous in the case of the C target since no plateau is devel-

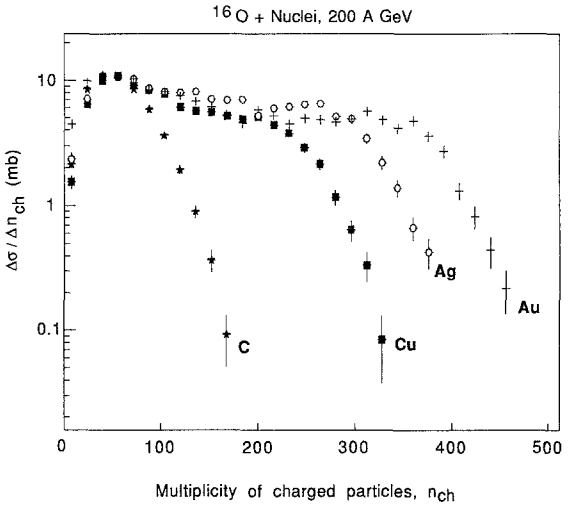

Fig. 2. Charged particle multiplicity distributions for 200 A GeV ^{16}O induced nuclear reactions with C, Cu, Ag, and Au targets in the pseudo-rapidity range $-1.7 < \eta < 4.2$

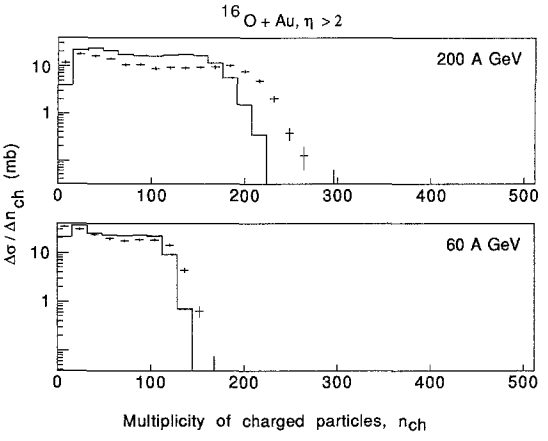

Fig. 3. Charged particle multiplicity distributions for 60 and 200 A GeV ^{16}O + Au interactions in the pseudo-rapidity range $2.0 < \eta < 4.2$ compared to predictions from the event generator FRITIOF [9]. The model predictions are given by the solid histograms

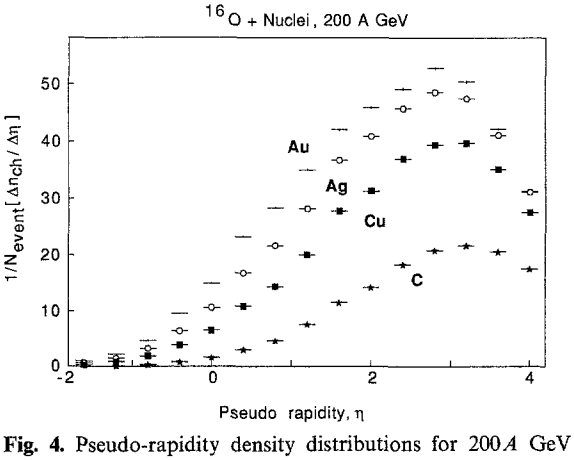

Fig. 4. Pseudo-rapidity density distributions for 200 A GeV ^{16}O induced nuclear reactions with C, Cu, Ag, and Au targets

oped and since the carbon nucleus is smaller than the oxygen nucleus) you find a target mass number dependence close to $A^{1/3}$. This supports the above geometrical picture where the length of the cylindrical volume passed by the projectile nucleus is proportional to the radius of the target nucleus.

In order to compare with the predictions from the FRITIOF event generator, in which the target spectator fragments are not included, we have restricted the multiplicity distributions to a region where the yield of such particles is believed to be small. In Fig. 3 we therefore present the multiplicity distributions at 60 and 200A GeV ^{16}O+Au interactions in the η region: $2.0<\eta<4.2$. The solid histograms represent the predictions from FRITIOF. The model predictions are normalized to the experimental cross-sections. We see that the simulations have not quite succeeded in reproducing the trigger bias since the deviations between the data and the generated events are large at the lowest multiplicities at both energies. The overall shapes of the model distributions do agree with the data but the model does not generate the high multiplicities of charged particles that are seen in the experiment. We have observed that the transverse energy for "central events", measured in the pseudo-rapidity interval $2.4<\eta<5.5$, are 10 to 15% higher than expected from FRITIOF calculations for all targets and projectile energies [11]. However, since the multiplicities of charged particles for these events also are 15–20% higher than in the model predictions the observation of higher E_t values is associated with an increase in the average particle production of the same order.

In order to give more detailed information about the charged particle yield we next turn to the pseudo-rapidity distributions. In Fig. 4 we show the pseudo-rapidity density distributions for all targets at the projectile energy 200A GeV. The position of the peak moves from about $\eta=2.7$ to $\eta=3.2$ (with an error of ± 0.1) as the target mass decreases. The position of the peak value of the "minimum-bias" pseudo-rapidity distribution hence moves backwards quite slowly with an increase in the target mass and stays close to the nucleon-nucleon centre-of-mass value of 3.0. The density of charged particles per unit of pseudo rapidity, at mid-rapidity values, increases from 22 to more than 50 as we go from the carbon to the gold target. In Fig. 5 we show the pseudo-rapidity density distributions at 200A GeV compared to the predictions from FRITIOF. The peak positions predicted by the model are at the same pseudo-rapidity values (within the errors) as the observed peaks. The particle density in the mid-rapidity region is underestimated by 20% for all targets. The deviations between data and model predictions that are seen in

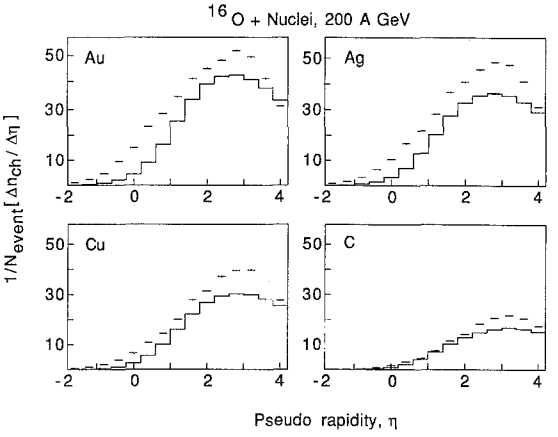

Fig. 5. Pseudo-rapidity density distributions for 200A GeV ^{16}O induced nuclear reactions with C, Cu, Ag, and Au targets compared to the predictions from FRITIOF. The model predictions are given by the solid histograms

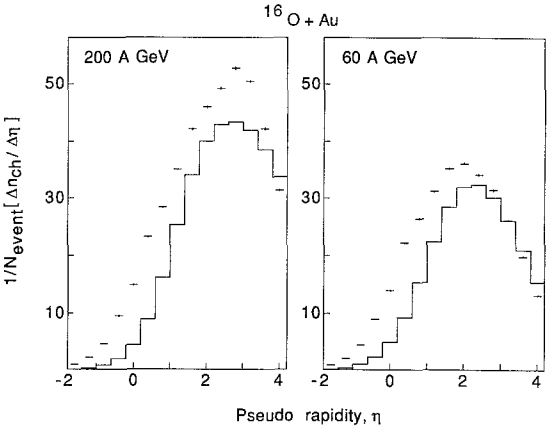

Fig. 6. Pseudo-rapidity density distributions for 60 and 200A GeV ^{16}O+Au interactions compared to FRITIOF. The predictions are given by the solid histograms

the target fragmentation region can qualitatively be explained by the fact that the target spectator fragments are not included in the model predictions. Furthermore, the model does not treat other more complex reaction mechanisms, such as cascading, that might be contributing in this region. As can be readily seen, the relative difference in the yield of charged particles in the latter region decreases with decreasing target mass.

In Fig. 6 we compare the pseudo-rapidity density distributions for ^{16}O+Au collisions at 60A GeV and 200A GeV with the predictions from FRITIOF. The particle production in the target fragmentation region is independent of the projectile energy. This is a well-known feature in hadron-nucleus collisions at relativistic energies and, as can be seen from the figure, this appears to be valid also in the case of nucleus-nucleus collisions. The absolute deviation between the data

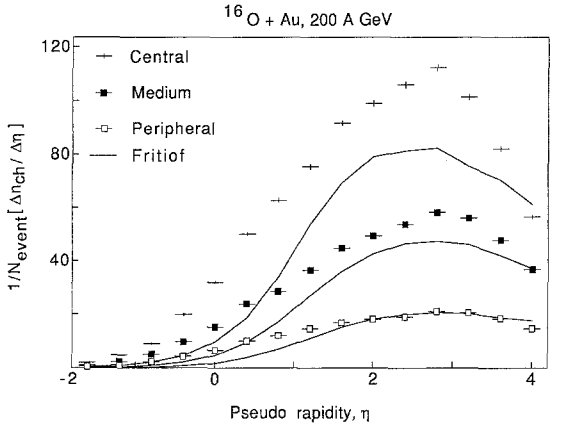

Fig. 7. Pseudo-rapidity density distributions for different classes of "centrality" for 200A GeV ^{16}O+Au interactions are compared to the predictions from FRITIOF. The events are classified by the energy within $\theta \leqq 0.3°$, E_{ZDC}, as measured in the uranium-plastic sampling calorimeter, ZDC: Central events: $E_{ZDC} < 300$ GeV; Medium events: 900 GeV $< E_{ZDC} \leqq 1700$ GeV; Peripheral events: $E_{ZDC} > 1700$ GeV

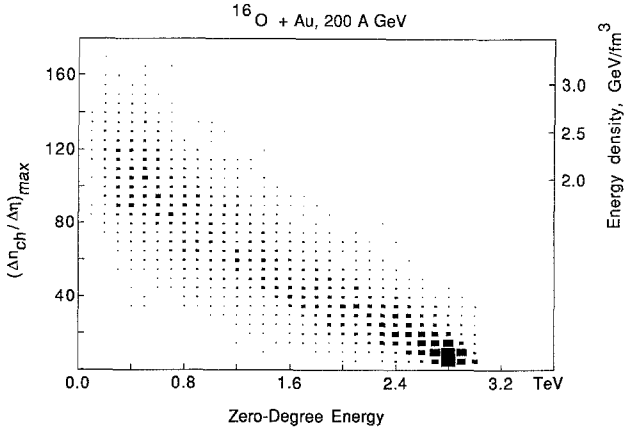

Fig. 8. The density of charged particles in the pseudo-rapidity interval $2.65 < \eta < 3.15$ for ^{16}O+Au at 200A GeV, $(\Delta n_{ch}/\Delta\eta)_{max}$, as a function of the energy measured in the ZDC, E_{ZDC}. On the scale to the right we show the corresponding energy densities, derived as described in the text

and the model is independent of energy up to mid-rapidity values. The model underestimates the data in the central region at 200A GeV projectile energy, whereas at the lower bombarding energy this difference is not so pronounced. However, in the case of the lower projectile energy the mid-rapidity region is so close to the target fragmentation region that it is impossible, using only the angular information, to classify the particles as originating from conceptually different production mechanisms.

The multiplicity of charged particles in an event strongly depends on the "centrality" of the collision. In this presentation we operationally define the "centrality" by making different cuts on the energy measured in the Zero-Degree Calorimeter (ZDC). In Fig. 7 we show the pseudo-rapidity density distributions for ^{16}O+Au at 200A GeV in three different energy bins. The first class of events are those where an energy of less than 300 GeV was measured by the ZDC. This group of events we will denote central events. The second and the third class of events were sampled in the bins where the energy in the ZDC was 900 GeV $< E <$ 1700 GeV and larger than 1700 GeV, respectively. These events we will call medium and peripheral events. In terms of percentage of the measured cross section the number of events in these classes correspond to 6, 22 and 47±2%. The solid histograms represent the distributions as given by FRITIOF. The average density of charged particles at mid rapidity is 110 for the central events, around 60 for the medium events and 20 in the case of peripheral events. The relative difference between the data and the model prediction at mid-rapidity values changes from close to zero for the peripheral events to around 30–35% for the central events. From the figure we can conclude that the model fails to describe the production of charged particles at mid-rapidity values and that the difference is larger for the more central events.

In Fig. 8 we display, event by event, the density of charged particles in the pseudo-rapidity interval $2.65 < \eta < 3.15$ for ^{16}O+Au at 200A GeV versus the energy measured in the ZDC. As one moves from the right to the left on the energy axis (x-axis), the more "central" the event becomes. It can be concluded that not only is the average charged particle density in this pseudo-rapidity interval high (up to 110) but the fluctuations around the average value are also large. In order to estimate the energy densities corresponding to these particle densities we give, on the right y-axis, those calculated by the formula [12]:

$$\varepsilon = \frac{3\langle m_t \rangle \Delta n_{ch}}{2\tau_0 A_t \Delta\eta};$$

where we have used $\tau_0 = 1$ fm/c, $\langle m_t \rangle = 370$ MeV, $A_t = \pi(1.2)^2(16)^{2/3}$, and have used 2:3 for the ratio of charged to all produced particles. It should be pointed out that such an estimate is only valid under the assumptions made within a hydrodynamical picture. Furthermore, there is no general agreement about what values one should use for τ_0 or A_t. The attained values should therefore only be used in relative comparisons with other experiments or as "order-of-magnitude" estimates rather than as absolute numbers for the energy densities achieved. With these precautions in mind, it is still interesting to note that we, with the use of this formula, reach values of the energy density of about 3 GeV fm^{-3}.

Summary and conclusions

We have presented charged multiplicity distributions and pseudo-rapidity density distributions of ^{16}O collisions with various target nuclei at 60 and 200 A GeV. The distributions were compared to predictions from the event generator FRITIOF. In the case of $^{16}O + Au$ interactions at 200 A GeV the observed multiplicity of charged particles reaches up to 450 for the most central events. The FRITIOF prediction fails to reproduce these high multiplicities. The position of the peak values of the minimum-bias pseudo-rapidity distributions at 200 A GeV, close to $\eta = 3$ for all targets, are correctly predicted by the model. At the higher bombarding energy, for all targets, the particle density at mid-rapidity values are 15–20% higher in the data than in the model predictions. The yield of charged particles in the target fragmentation region is seen to be independent of the projectile energy. The particle density depends strongly on the centrality of the collision. The average particle density at mid-rapidity values, in the case of $^{16}O + Au$ interactions at 200 A GeV, reaches a value of 110 for the central collisions. The fluctuations around this average value are large and, using a hydrodynamical picture of the collision, energy densities up to 3 GeV fm^{-3} are calculated.

References

1. Faessler, M.A.: Phys. Rep. 115 (1984) 1; Shuryak, E.V.: Phys. Rep. 61 (1980) 71
2. See also Bamberger, A. et al.: Phys. Lett. 184 B (1987) 271
3. Gutbrod, H.H. et al.: Proc. 15th Int. Workshop on Gross Properties of Nuclei and Nuclear Excitations, Hirschegg, Kleinwalsertal, Austria, 1987, H. Feldmeier (ed.), Darmstadt, Report ISSN 0720-8715 (1987) 42; Albrecht, R. et al.: GSI Scientific Report 1986 No. GSI-87-1, (1987) 77-85
4. Awes, T.C. et al.: (To be published). Not published yet
5. Baden, A. et al.: Nucl. Instrum. Methods 203 (1982) 189
6. Albrecht, R et al.: GSI-Darmstadt Report No. GSI-85-32, 1985; Iarrocci, E.: Nucl. Instrum. Methods 217 (1983) 30
7. Bell, W. et al.: Z. Phys. C – Particles and Fields 27 (1985) 191
8. Andersson, B., Otterlund, I., Stenlund, E.: Phys. Lett. 84 B (1979) 470
9. Nilsson-Almqvist, B., Stenlund, E.: Comp. Phys. Commun. 43 (1987) 387
10. Andersson, B., Gustafson, G., Nilsson-Almqvist, B.: Nucl. Phys. 281 B (1987) 289
11. Albrecht, R. et al.: Phys. Lett. B 199 (1987) 297
12. Cleymans, J., Gavai, R.V., Suhonen, E.: Phys. Rep. 130 (1986) 217; Bjorken, J.D.: Phys. Rev. D 27 (1983) 140